# STCALC - A HYPERSONIC SHOCK TUNNEL CALCULATOR

**Mauricio A. P. Rosa, pinheiro@ieav.cta.br**
**Francisco D. Rocamora Jr., junior@ieav.cta.br**
**Artur C. Menezes, arturm@ieav.cta.br**
Instituto de Estudos Avançados (IEAv), Rodovia dos Tamoios, km 5,5 – Putim – CEP 12228-001, São José dos Campos, SP

**Abstract.** The main objectives of this work are to present the models and methods implemented in a new version of a computational tool for the calculations of air flow properties, which are not or cannot be measured directly in the experiments with pulsed hypersonic shock tunnels, as well as to present several numerical and experimental results. New numerical strategies have been used in this new version of the program in order to overcome some result inconsistency observed in the calculations with the previous version for the air chemical and thermodynamic equilibrium model. The results presented herein have mainly the purpose of code verification and validation and have demonstrated that the STCALC program can be used to predict with good accuracy the airflow parameters inside pulsed hypersonic shock tunnels.

*Keywords*: *shock tunnel, hypersonics, numerical simulation*

## 1. INTRODUCTION

Design of hypersonic vehicles, both the spatial ones that return to earth as well as the ones that remain in the atmosphere depend on a variety of laboratory test results that simulate as close as possible the projected flight regimes. In this context, pulsed hypersonic shock tunnels are very powerful tools used for simulating in laboratory, for a short period of time, airflows above Mach 6 with properties similar to the ones of high altitude atmospheres (Toro, 2006; Minucci et al., 2007). Basically, these devices are constituted of a shock tube coupled to a convergent-divergent nozzle whose exit is inside of a closed test section. The shock tube produces a highly compressed gas at the nozzle inlet, which expands and accelerates inside the nozzle leaving it at hypersonic speeds inside a test section where hypersonic models are placed to be analyzed.

The Aerothermodynamics and Hypersonic Laboratory (LAH) at the Instituto de Estudos Avançados (IEAv) has several pulsed hypersonic wind tunnels, which differ from one another mainly in the size, test time and flow speeds in the test section. Presently, in this laboratory, it is possible to simulate flows up to Mach 25, approximately, where a variety of experiments have already been performed and others are now underway, using the hypersonic wind tunnels.

For the analysis of the results of a shock tunnel experiment, it is very important to have a good knowledge of the hypersonic flow stream that the body in analysis is facing. In a standard hypersonic shock tunnel, due to intrinsic limitations in flow measurements, this is only possible by numerically solving theoretical mathematical models of the gas flowing inside the several parts of the shock tunnel. In other words, flow parameters, which are not, or cannot be, directly measured, are then calculated from theoretical models.

In a previous work (Rosa et al., 2008), it was presented models and methodologies as well as input and output graphical interfaces adopted in the development of a shock tunnel calculator to be used mainly as an auxiliary tool for experimentalists. During the verification and validation processes using the "real" gas model calculations, it was observed some inconsistency of the results, mainly for the low nozzle inlet enthalpy conditions, which was later on verified to be caused only by inaccuracies of some polynomial functions obtained by curve fittings. These polynomials relate the air thermodynamics properties considering it in chemical and thermodynamic equilibrium for temperatures up to 25,000 K (Srinivasan et al, 1987).

The main objective of this work is to present the new models and numerical strategies used to overcome the problems mentioned above although still using the Srinivasan's correlations. Also, it will be presented some new calculations added to the program as well as validation results for this new version. This new version of the shock tunnel simulator has been named as STCALC (Shock Tunnel CALCulator), developed for parameter estimates of gas flows inside hypersonic shock tunnels

## 2. PULSED HYPERSONIC SHOCK TUNNELS

This section has the purpose of briefly explain how a pulsed hypersonic shock tunnel works. Figure 1 shows schematically the most important parts of such a tunnel, i.e., the shock tube, the nozzle, the test section, the model and the dump tank as well as the locations of the pressure sensors.
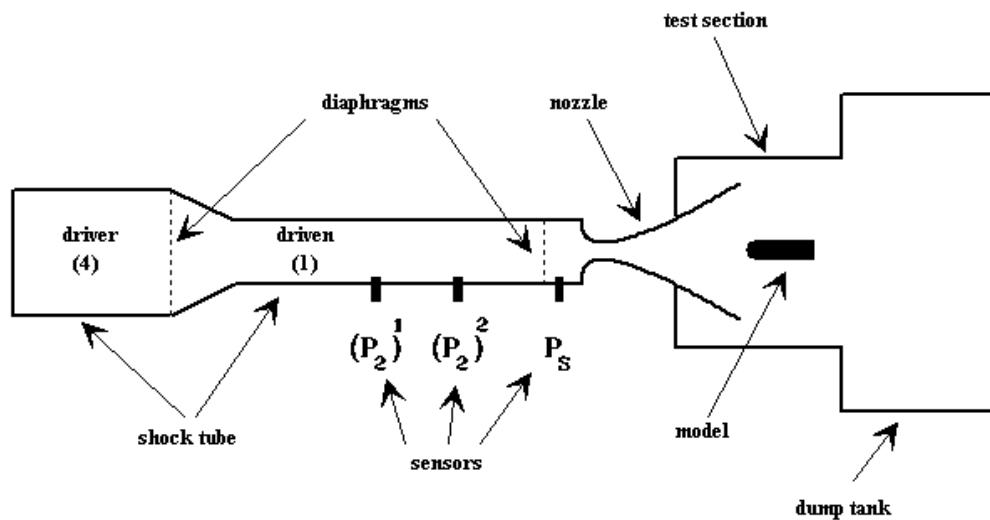
Figure 1. A pulsed hypersonic shock tunnel schematic.

The shock tube is initially divided in two regions by a diaphragm, named as driver (region "4") and driven (region "1"). The driver is filled with a very high-pressure gas, usually helium or air, and the driven is filled with a low-pressure gas, usually air. The driven end is connected to the entrance of a convergent-divergent nozzle whose exit is located inside the test section where a model is placed for analyses. The shock tube and the nozzle are initially separated by another diaphragm. When the driver-driven diaphragm is ruptured, expansion waves move to the left into the driver and a shock wave, named as incident shock wave, moves to right into the driven leaving behind a region ("2") with increased temperature and pressure, as can be seen in Fig. 2.
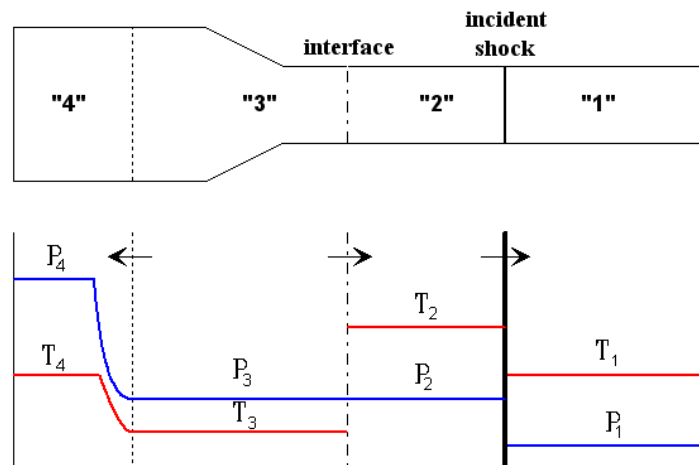


Figure 2. Pressure and temperature inside the shock tube a short while after diaphragm rupture.

When the incident shock wave reaches the end of the driven, it is reflected back into the driven leaving behind it a region ("5") with even higher pressure and temperature in almost stagnation condition, as shown in Fig. 3. By this time the driven-nozzle diaphragm has been ruptured and this compressed and high temperature driven gas starts flowing into the nozzle where it expands, consequently decreasing pressure and temperature, and accelerates in the direction of the nozzle exit leaving it with hypersonic speeds (Mach 5 or higher). This high speed free stream flow then reaches the model where after a very short while a shock wave is formed over the body, as shown schematically in Fig. 4. This hypersonic flow condition persists only for a short period of a few milliseconds.
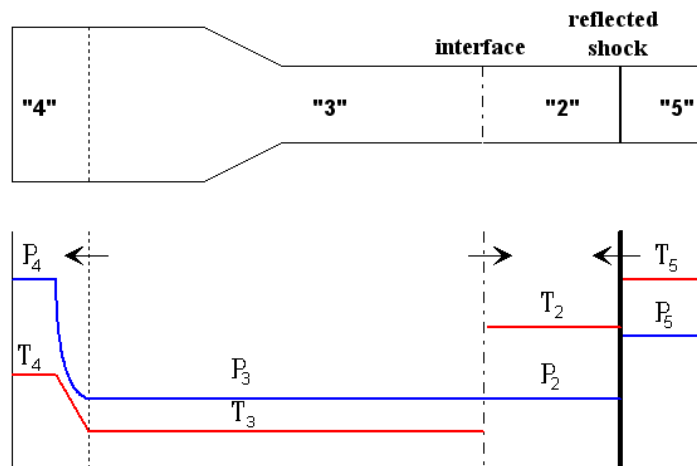
Figure 3. Pressure and temperature inside the shock tube a short while after the incident shock has reflected back at the nozzle entrance.
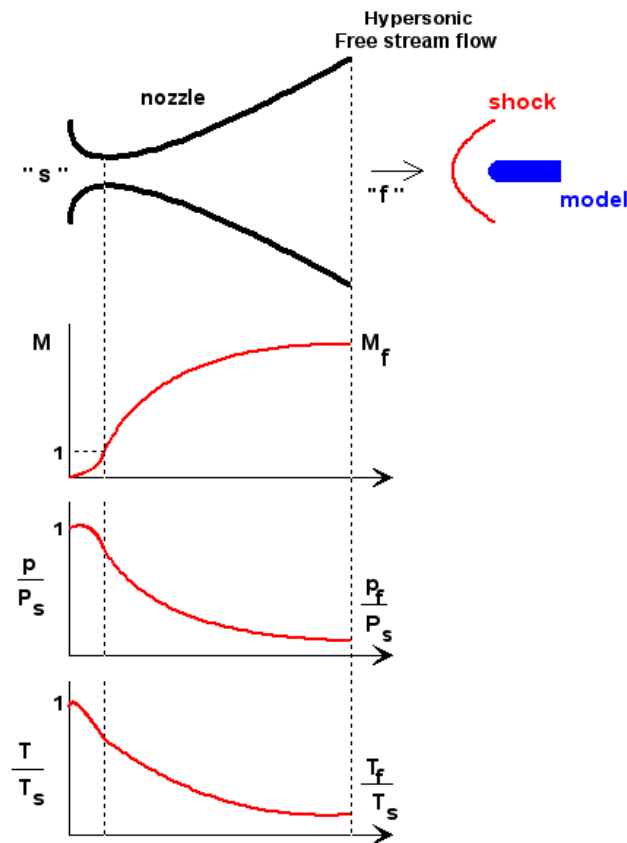


Figure 5. A schematic of the nozzle and the model in the test section showing also the Mach number, pressure and temperature variation inside the nozzle.

The first two pressure sensors, shown in Fig. 1, $(P_2)^1$ e $(P_2)^2$, are used for measuring the incident shock wave transit time between them and, consequently, for estimating the incident shock wave velocity. The other sensor at the end of the driven, $P_S$, is used for measuring the nozzle-supply pressure. Although it is not shown in this figure, usually a pressure sensor is placed at the tip of the model (stagnant point). The STCALC program needs all these information to calculate the flow parameters in the tunnel.

## 3. MODELS AND METHODS

The STCALC program calculations do not depend directly on the driver gas initial conditions since the measured incident shock wave transit time is used to calculate the shock wave velocity. The models implemented in the program consider only the calculations of the first reflection of the incident shock wave at the nozzle entrance. This model limitation for cases for which there is more then a single reflection, such as, for instance, when the tunnel operates in the interface equilibrium mode, is overcome by the possibility of providing the code the measured nozzle-supply pressure.

Two distinct models have been incorporated to the program for the airflow in the tunnel: a) the calorically perfect; and b) the chemical and thermodynamic equilibrium air models. The former model uses analytical thermodynamics relationships, which are widely available in the literature (Anderson, 1990). The latter model uses complex polynomial functions relating a single air thermodynamic property to any other two properties. These polynomial functions are obtained from curve fittings presented in Srinivasan et. al. (1987), which are valid for temperatures up to 25,000 K. For this model, a subroutine library for the following functions is available in the STCALC program:

$$P = P(\rho, e), \quad a = a(\rho, e), \quad T = T(\rho, e), \quad s = s(\rho, e),$$
$$\rho = \rho(P, s), \quad e = e(P, s), \quad a = a(P, s),$$
$$e = e(P, \rho), \quad T = T(P, \rho), \quad h = h(P, \rho)$$

where: $P$ is pressure, $\rho$ is density, $e$ is internal energy, $a$ is sound speed, $T$ is temperature, $s$ is entropy, $h$ is enthalpy.

The models for shock tube calculations also consider that the shock waves, both incident and reflected, are normal to the flow direction, therefore, they can be treated as one-dimensional models.

Two methods for the nozzle and test section calculations are implemented in the program: a) one that considers the nozzle geometry in terms of the divergent-throat area ratio; and b) other one that considers the measured stagnant pressure at the nozzle exit (or sensor contact pressure).

Although it is possible, and not wrong, to use any combination of the Sirinivasan's correlations available in the subroutine library to calculate the air properties (Rosa et. al, 2008), it was observed during the program verification and validation processes that this procedure would lead, in some situations, to lack of result consistency due to the fact that some correlations are considerably more imprecise than others. In other words, different ways, or group of correlations, to calculate a specific property may lead to considerable different results, which, in some cases, can be also very inconsistent. To overcome this problem, from the original set of correlations presented above, a reduced set of more precise correlations was taken for all calculations in the program, that is:

$$P = P(\rho, e), \quad a = a(\rho, e), \quad T = T(\rho, e), \quad s = s(\rho, e), \quad h = h(P, \rho)$$

As a penalty to this was the need to develop several iterative algorithms for the calculations of these properties since, in many circumstances, one of the two properties available for using a specific correlation was the dependent variable and one of the independent variables was unknown. This procedure has been adopted for all calculations in this new version of the program, although different algorithms had to be developed for each specific calculation.

In the following sections will be presented the calculation methods for the chemical and thermodynamics equilibrium air model only. The calorically perfect gas model uses analytical expressions, which are available in literature (Anderson, 1990), so it will not be treated here.

### 3.1 Incident Shock Wave

Figure 6 shows the incident shock wave in the "laboratory" and "stationary shock" frames. The air in the driven is initially stagnant, but as the shock wave passes a velocity is induced to the air behind it. In the "stationary shock" frame, the conditions of the air in region "1" are known and the conditions behind the shock, in region "2", are to be calculated. In this frame, the velocities entering and leaving the shock are $u_1 = u_i$ an $u_2 = u_i - u_g$, respectively, where $u_i$ is a known incident shock velocity and $u_g$ is the unknown induced air velocity behind the shock. So, the flow behind the shock properties (region "2") can be calculated from the mass, momentum and energy conservation equations for a normal shock and two more auxiliary equations giving the thermodynamics description, which can be cast into the form:

$$u_2 = \frac{\rho_1 u_1}{\rho_2}$$

$$P_2 = P_1 + \rho_1 u_1^2 (1 - \frac{\rho_1}{\rho_2})$$

$$h_2 = h_1 + \frac{u_1^2}{2}\left[1 - \left(\frac{\rho_1}{\rho_2}\right)^2\right]$$

$$e_2 = h_2 - \frac{P_2}{\rho_2}$$

$$P_2 = P(\rho_2, e_2)$$

Differently from the program previous version (Rosa et. al, (2008)), which used a functional minimization procedure to solve the above nonlinear equations (O'Neill, R., 1971), this new version uses an iterative procedure calculation presented in Anderson (1989). This was necessary because the minimization procedure has failed to converge to some specific precision requirements in some situations whereas the present iterative method has been consistent always.
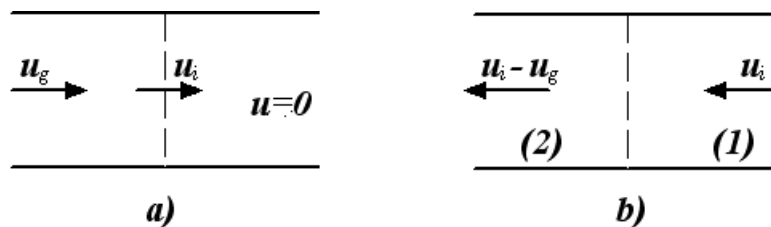


Figure 6. Incident shock wave in the a) "laboratory" and "stationary shock" frames.

For each iteration, the density $\rho_2$ is known a priori, then the variables $u_2$, $h_2$, and $P_2$ are calculated from the conservation equations. The auxiliary equations are then used for the calculations of $e_2$ and the pressure, $P_2'$. If $P_2 \approx P_2'$, then the process is stopped and $u_g$ is calculated, otherwise, a new value for the density is provided and the process is repeated. For the first two iterations, the density is simply guessed, but from the third iteration on the density is calculated using the Secant Method for $\Delta P = P_2 - P_2'$ and $\rho_2$.

**3.2 Reflected Shock Wave**

Figure 7 shows the reflected shock wave in the "laboratory" and "stationary shock" frames. In the "stationary shock" frame, the conditions of the air ahead of the shock (region "2") are already known and the conditions behind the shock, in region "5", are to be calculated. In this frame, the velocities entering and leaving the shock are $u_2 = u_r + u_g$ and $u_5 = u_r$, respectively, where $u_r$ is the unknown reflected shock velocity and $u_g$ is already known. So, the flow behind the shock properties (region "5") and the reflected shock velocity can be calculated from the mass, momentum and energy conservation equations and auxiliary equations giving the thermodynamics description, which can be cast into the form:

$$u_r = \frac{\rho_2 u_g}{\rho_5 - \rho_2}$$

$$P_5 = P_2 + \rho_2 u_g^2 \left(\frac{\rho_5}{\rho_5 - \rho_2}\right)$$

$$h_5 = h_2 + \frac{u_g^2}{2}\left(\frac{\rho_5 + \rho_2}{\rho_5 - \rho_2}\right)$$

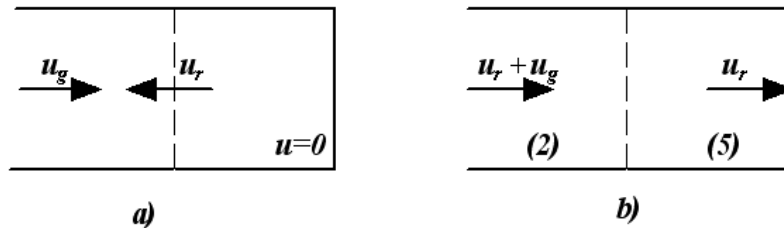$$e_5 = h_5 - \frac{P_5}{\rho_5}$$

$$P_5 = P(\rho_5, e_5)$$



Figure 7. Reflected shock wave in the a) "laboratory" and "stationary shock" frames.

From $u_g$, $\rho_2$, $h_2$, $e_2$ and $P_2$, the flow properties behind the reflected shock $\rho_5$, $h_5$, $e_5$, and $P_5$ as well the velocity $u_r$ can be calculated from the above equations using the same iterative procedure described before for the incident shock.

### 3.3 Nozzle

The nozzle-supply conditions "S" (see Fig. 4), in the STCALC program, can be either the ones calculated for region "5" or the pressure can be given as input so that the measured pressure, $P_S$, can used if wished. In the latter case, to obtain the other air properties, it is assumed an isentropic expansion or compression from state "5" to pressure $P_S$ so that $s_S = s_5$. These two parameters along with the reduced set of correlations have been used to iteratively calculate the remaining properties. The airflow velocity at the nozzle entrance is very small so that it may be considered in stagnation, i.e., $u_S = u_5 \approx 0$, so the total enthalpy is given by: $H_S = e_S + P_S/\rho_S$.

The models consider that the entire tunnel system is adiabatic so that the total enthalpy remains the same everywhere and also that the air expands isentropically in the nozzle. Besides these conditions, the flow properties at the nozzle throat are obtained, again iteratively, using the sonic flow condition also, i.e., $u_T = a_T$. Differently from in the program previous version , the reduced set of correlations mentioned before is used here.

The free stream flow at the nozzle exit can be calculated using two distinct methodologies: one considers the nozzle geometry, more specifically, the divergent-to-throat area ratio; and the other uses the measured contact (stagnation) pressure of a sensor with a blunt body shape placed axially on the nozzle symmetry axis, as shown schematically in Fig. 5. In the former methodology, the nozzle exit pressure is decreased in small steps until it is observed mass conservation between the nozzle throat and exit. The latter methodology is based on that described in Minucci (1991) and it is different from the one implemented in the previous version. On the symmetry axis it is assumed a normal shock on the sensor, as shown in Fig. 5. The entropy changes in the normal shock but it remains the same within the shock layer. First, this entropy is calculated from the enthalpy (total enthalpy) and the sensor measured pressure. Next, the free stream flow conditions are varied, using again an iterative procedure, until the calculated behind normal shock entropy (see the incident shock wave model) matches the one calculated for the stagnation condition on the sensor. At this point, the free stream flow and the sensor contact properties are already known. Using the same modeling, the sensor contact properties are calculated in the former methodology too, except that, in this case, the free stream flow is already established.

### 4. ANALYSIS OF RESULTS

Several numerical results obtained with the new version of the hypersonic shock tunnel calculator, STCALC, have been compared with both experimental and numerical results from other computer programs for the purpose of program validation. Although the STCALC program performs calculations for both calorically perfect ("perfect gas") and chemical and thermodynamics equilibrium ("real gas") models for the air in the driven, here will be presented validation results only for the latter case, which is more realistic, although the "perfect gas" model has also been validated against analytical calculations. The validation results presented here will be presented separately for the shock tube and nozzle parts of tunnel. This was necessary because most of the results found in the literature were for shock tubes and nozzles separately.

The results for the shock tube calculations with the STCALC program have been compared with the respective ones obtained from other codes, such as G.E., AVCO, CALSPAN and HSTR as in Minucci, 1991. Table 1 shows the results for pressure, temperature and density behind the incident and the reflected shock waves in the shock tube for different sets of initial driven air pressure and temperature and incident shock wave Mach number. As can be seen the results are close to each other and the difference may be due to these codes use different chemical and termodynamics equilibrium air property sources. Table 2 shows the results obtained from both experiments (Menezes et al., 2009) and calculated with the STCALC program for the pressure behind of the reflected shock wave resulting from the reflection of the incident shock wave at the nozzle inlet, i.e., the end of the shock tube. Several experimental runs were performed with the T2 hypersonic shock tunnel of the LAH at the IEAv with both helium and air in the driver at 3,000 psi pressure and ambient temperature for air initial conditions in the driven of 96 and 288 kPa pressure and ambient temperature. The resulting incident shock wave Mach numbers are also shown in this table. Figure 8 shows, as examples, typical nozzle-supply pressure sensor responses obtained in experiments with helium gas and air in the driver for a 288 kPa initial driven pressure. The fast pressure growth seen in these responses refer basically to time instant the incident shock wave reaches the end of the tube and is reflected back. So, the first part of the response corresponds to the measured pressure behind the reflected shock wave. The remaining parts of the responses are not shown in these plots for the sake of clarity. The mean values calculated from these responses are then taken as the reflected pressure and, in these specific cases, as the nozzle-supply pressure too. In Table 2 are also shown these mean values and the respective standard deviations. As can be seen, the measured and STCALC calculated reflected pressure results agree quite well since they are basically within their respective standard deviation values.

Table 1. Incident and reflected shock wave results, for different shock tube initial conditions, calculated with the STCALC and similar computer codes.

| STCALC Computer Code Validation – SHOCK TUBE | | | | | | | | | |
|---|---|---|---|---|---|---|---|---|---|
| Input | | | | Output | | | | | |
| | | | | Behind incident shock | | | Behind reflected shock | | |
| Source | $P_1$ (kPa) | $T_1$ (K) | $M_S$ | $P_2$ (MPa) | $T_2$ (K) | $\rho_2$ (kg/m3) | $P_5$ (MPa) | $T_5$ (K) | $\rho_5$ (kg/m3) |
| G.E. | 0.0148 | 298.15 | 16.4 | ------- | 5,870 | 0.00189 | ------ | ------- | ------- |
| HSTR | 0.0148 | 298.15 | 16.4 | 0.005 | 5,388 | 0.00240 | 0.08 | 7,521 | 0.0207 |
| STCALC | 0.0148 | 298.15 | 16.4 | 0.005 | 5,406 | 0.00239 | 0.08 | 7,479 | 0.0206 |
| AVCO | 1.33 | 300 | 14.4 | 0.360 | 5,880 | 0.167 | 4.40 | 8,640 | 1.153 |
| HSTR | 1.33 | 300 | 14.4 | 0.353 | 5,746 | 0.169 | 4.43 | 8,599 | 1.170 |
| STCALC | 1.33 | 300 | 14.4 | 0.351 | 5,828 | 0.167 | 4.36 | 8,571 | 1.156 |
| CALSPAN | 1.33 | 293.15 | 10.6 | ------- | ------- | ------- | 2.07 | 6,720 | ------- |
| HSTR | 1.33 | 293.15 | 10.6 | 0.189 | 3,849 | 0.153 | 2.16 | 6,657 | 0.877 |
| STCALC | 1.33 | 293.15 | 10.6 | 0.189 | 3,829 | 0.152 | 2.14 | 6,601 | 0.886 |
| HSTR | 5 | 300 | 6.0 | 0.215 | 2,109 | 0.351 | 1.588 | 3,416 | 1.540 |
| STCALC | 5 | 300 | 6.0 | 0.216 | 2,100 | 0.356 | 1.619 | 3,470 | 1.565 |
| HSTR | 25 | 300 | 5.0 | 0.742 | 1,590 | 1.612 | 5.137 | 2,803 | 6.273 |
| STCALC | 25 | 300 | 5.0 | 0.742 | 1,591 | 1.612 | 5.136 | 2,819 | 6.284 |
| HSTR | 100 | 300 | 4.0 | 1.883 | 1,139 | 5.709 | 11.714 | 2,047 | 19.766 |
| STCALC | 100 | 300 | 4.0 | 1.879 | 1,150 | 5.644 | 11.524 | 2,030 | 19.618 |
| HSTR | 300 | 300 | 3.0 | 3.135 | 783 | 13.951 | 15.88 | 1,302 | 42.130 |
| STCALC | 300 | 300 | 3.0 | 3.127 | 781 | 13.821 | 15.71 | 1,308 | 41.478 |

Table 2. Behind reflected shock wave pressures from experiments and STCALC calculations.

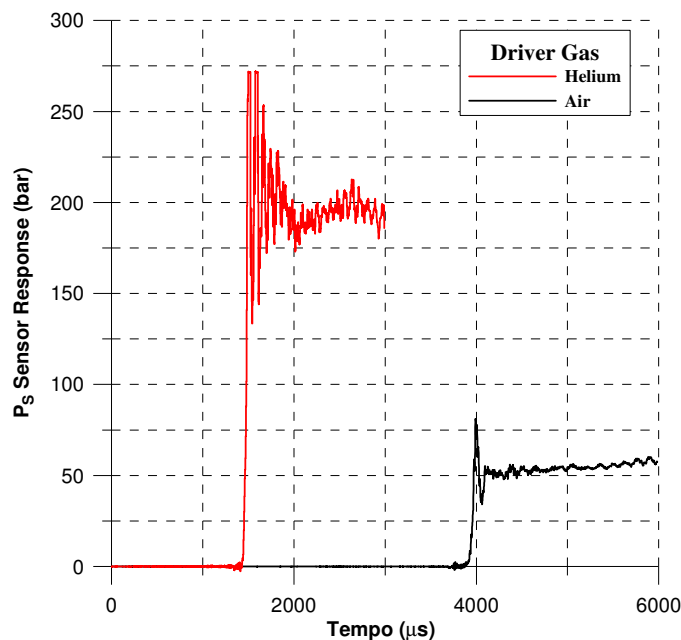| STCALC Computer Code Validation – SHOCK TUBE | | | | | | |
|---|---|---|---|---|---|---|
| **Input** | | | | **Output** | | |
| | | | | **First Reflection Pressure:** $P_5$ (MPa) | | |
| | | | | **Calculated** | **Measured** | |
| **Driver gas** | $P_1$ (kPa) | $T_1$ (K) | $M_S$ | **STCALC** | **Mean** | **Standard deviation** |
| Helium | 288 | 295 | 3.365 | 20.83 | 19.51 | 2.29 |
| Helium | 96 | 295 | 4.171 | 12.32 | 13.87 | 1.31 |
| Air | 288 | 295 | 2.140 | 5.38 | | 0.33 |
| Air | 96 | 295 | 2.456 | 2.77 | | 0.19 |



Figure 8. Typical nozzle-supply pressure sensor responses from experiments at the T2 shock tunnel.

Next, some STCALC validation results will be presented for the nozzle part of the tunnel. Table 3 presents some important properties of the free stream flow at nozzle exit calculated with the STCALC and others already validated computer programs, such as, CALSPAN, G.E., NACA and NOZZLEFLOW as in Minucci (1991), for specific nozzle geometries and nozzle-supply pressure and temperature conditions. As can be noticed from the results in this table, the results from the STCALC program agree very well with the ones obtained with other codes if it is taking into account that, as already mentioned, these codes may use different sources for the chemical and thermodynamics equilibrium air properties. From these results, it can also be observed that pressure and temperature calculated with STCALC are always a little bit lower than the ones calculated with the NOZZLEFLOW program, which uses the Tannehill & Mugge, (1974) correlations for air properties instead. Also, in Fig. 9, pressure calculations at nozzle exit with the STCALC program are compared against experimental results from Nagamatsu & Sheer as in Minucci (1991). As can be observed, there is a very good agreement between the results from experiments and the ones calculated with the STCALC program. The discrepancies between the numerical and the experimental results observed in this figure for nozzle-supply temperatures higher than 4,500 K are due to air nonequilibrium effects which become important for such high temperatures and the models in the STCALC program are only for equilibrium air.

Table 3. Free stream flow properties calculated with the STCALC program and others already validated codes.

| Sources | Input | | | Output | | | |
|---|---|---|---|---|---|---|---|
| | $P_0$ (MPa) | $T_0$ (K) | $A_D / A_t$ | $P_f$ (kPa) | $T_f$ (K) | $\rho_f$ (kg/m$^3$) | $u_f$ (m/s) |
| CALSPAN | 99,01 | 4.000 | 10 | 1,020 | 1,606 | 2.197 | 2,699 |
| NOZZLEFLOW | 99,01 | 4.000 | 10 | 1,100 | 1,698 | 2.247 | 2,699 |
| STCALC | 99,01 | 4.001 | 10 | 1,050 | 1,612 | 2.241 | 2,688 |
| CALSPAN | 99,01 | 4.000 | 1,000 | 1.67 | 247 | 0.0195 | 3,200 |
| NOZZLEFLOW | 99,01 | 4.000 | 999.5 | 1.70 | 316 | 0.0187 | 3,205 |
| STCALC | 99,01 | 4.000 | 1,000 | 1.53 | 282 | 0.0188 | 3,199 |
| G.E. | 3,45 | 4.000 | 576 | 0.142 | 450 | ***** | ***** |
| NOZZLEFLOW | 3,45 | 4.000 | 576 | 0.147 | 491 | 0.00104 | 3,341 |
| STCALC | 3,45 | 4.000 | 576 | 0.138 | 458 | 0.00105 | 3,344 |
| NACA | 0.69 | 500 | 143.6 | 0.105 | 40.6 | 0.00904 | ***** |
| NOZZLEFLOW | 0.69 | 500 | 143.6 | 0.104 | 40.3 | 0.00901 | 961 |
| STCALC | 0.69 | 500 | 143.6 | 0.094 | 41.1 | 0.00795 | 968 |
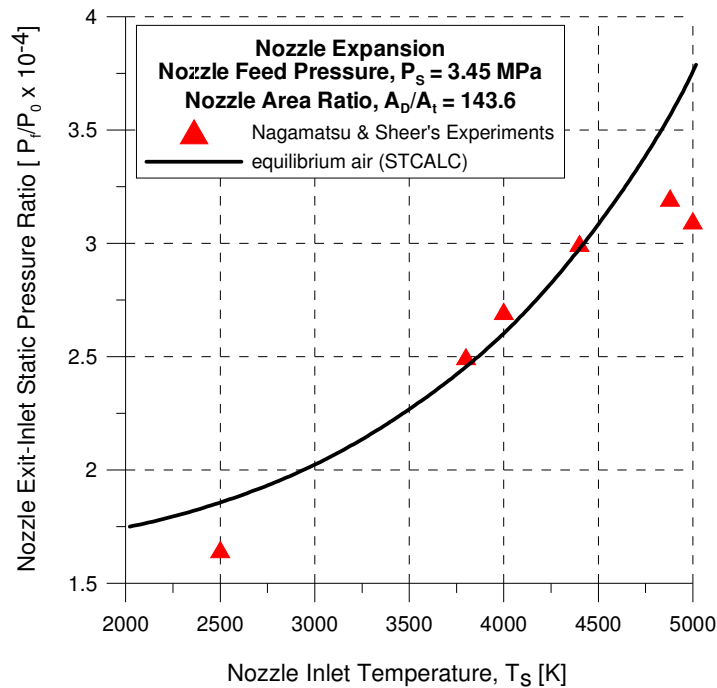


Figure 9. Experimental and STCALC calculated exit nozzle free stream flow static pressure.

The results presented in this section confirm that the models and the methods implemented in the STCALC computer program can predict with good accuracy the flow properties in both the shock tube and nozzle exit in the test section of shock tunnels for nozzle reservoir temperatures up to 4,550 K, approximately.

## 5. FINAL COMMENTS

The models and numerical methods as well as some added calculations implemented in the new version of the hypersonic shock tunnel calculator program have been presented. Also, several comparison results of the STCALC program with others already validated computer programs as well as with experimental ones have showed quite good agreement, which demonstrate that the STCALC program can be used to predict with good accuracy the main air flow parameters inside pulsed hypersonic shock tunnels.

The STCALC program presented here is more suitable for analyses post experiments since it needs as input a few measured parameters, such as incident shock transit time, nozzle-supply pressure and sensor contact pressure in the test section. Nevertheless, in many circumstances, one wishes to know with a good accuracy the free stream flow parameters in the test section before running the experiment. For this purpose, it is being developed a simulator specifically for the T2 tunnel at IEAv, which does not require measured parameters as input, at least, explicitly. This has been possible with the help of a measured parameters data bank obtained from a series of experimental runs with the T2 tunnel (Menezes et al. 2009) from where it can be derived fitting curves for these measured parameters as function of tunnel parameters which are set before the experiment.

## 6. ACKNOWLEDGEMENTS

## 7. REFERENCES

Anderson, J. D., 1990, "Modern Compressible Flow: with Historical Perspectives", McGraw-Hill, New York.

Anderson, J. D., 1989, "Hypersonic and High Temperature Gas Dynamics", McGraw-Hill, New York.

O'Neill, R., 1971, "Algorithm AS47. Function Minimization Using a Simplex Algorithm", Applied Statistics, 20:338-345.

Menezes, A . C., Rosa, M. A. P., Rocamora, F. D., 2009, "Determinação de novas condições de ensaio do túnel hipersônicoT2 para o veículo SARA", Relatório Final do Programa UNIESPAÇO da AEB, to be published.

Minucci, M. A. S., Toro, P. G. P., 2007, "Túneis de Choque Hipersônicos", Scientific American-Brasil, nº 57.

Minucci, M. A. S., 1991, "An Experimental Investigation of a 2-D Scramjet Inlet at Flow Mach Numbers of 8 to 25 and Stagnation Temperatures of 800 to 4,100 K", Ph.D. Thesis, RPI.

Rosa, M. A. P., Rocamora, F. D., Menezes, A. C., 2008, "Um Programa Computacional para Cálculos de Escoamentos em Túneis de Choque Hipersônicos". In: Congresso Nacional de Engenharia Mecânica - CONEM2008, Salvador. v. 1. p. 100.

Srinivasan, S., Tannehill, J. C., Weilmuenster, K. J., 1987, "Simplified Curve Fits for the Thermodynamics Properties of Equilibrium Air", NASA Reference Publication 1181.

Tannehill, J. C. and P. H. Mugge, 1974, "Improved Curve Fits for the Thermodynamics Properties of Equilibrium Air Suitable for Numerical Computation Using Time-Dependent or Shock Capturing Methods", NASA CR-2470,.

Toro, P. G. P., 2006, "Aerotermodinâmica de Veículos Espaciais em Reentrada Atmosférica", Relatório Final do Programa UNIESPAÇO da AEB.

## 5. RESPONSIBILITY NOTICE

The authors are the only responsible for the printed material included in this paper.